

## DIGITAL DIAGNOSTICS OF MULTIPHASE FLOWS BY THE PATTERN RECOGNITION TECHNIQUES

E.V. Vorozhtsov, V.P. Kiselev, and S.P. Kiselev

Institute of Theoretical and Applied Mechanics SB RAS,  
630090 Novosibirsk, Russia

### Introduction

Both experimental techniques and numerical modeling can be applied to study the same hydrodynamic processes. As was noted in [1], the development and verification of the diagnostics methods often prove to be the most laborious part of the numerical experiment as in the laboratory experiment. The diagnostics usually involve the processing of the results, for example, the computation of integral characteristics, the distribution of the pressure coefficient  $C_p$  along the aircraft wing surfaces, plotting the isolines, etc. These diagnostics are made with the aid of corresponding computer codes, which enable one to relate the discrete variables of modeling to the quantities, which are easier to interpret or compare with theory or experiment.

The problems related to the experimental diagnostics prove to be more difficult than in the case of the diagnostics of the numerical modeling results. The numerical experiment diagnostics can indeed be carried out without any connection with the basic computations, whereas the laboratory measurements usually introduce the disturbances in experiment. The probes can alter the local flow, absorb the heat from the medium. On the other hand, in the numerical experiment, there is a problem of the tyranny of numbers: what to do with the dozens or hundreds of thousands of numbers obtained at the output of the numerical experiment?

The localization of various singularities in the flow: shock waves, slip lines, etc. is one of the problems of the interpretation of numerical results in aerodynamics. Previously a theory was presented in [2, 3], which enables one to assess the accuracy of the shock wave localization, for example, by maximum of the flow velocity gradient. It turned out that the divergence property of an employed finite-difference scheme is one of the necessary conditions for ensuring a small error of various gradient techniques for shock localization, or the differential analyzers, as they were termed in [2, 3]. Then it is possible to prove, under certain additional conditions, the existence and uniqueness of such a point in the zone of a smeared shock wave, the finite-difference shock wave center, whose location coincides with the exact location of the shock wave front. In the case of non-divergence difference schemes, the numerical experiments in [1 – 4] have shown that the error in shock wave front localization may be significant and even be a quantity of the order  $O(1)$ .

Thus, a theoretical base was formulated in [2, 3] for constructing such algorithms for shock localization in numerical solutions, which possess the convergence, that is their error tends to zero as the grid steps are refined.

Another problem, which often emerges at the investigation of the shockwave structure of flows on the basis of numerical experiment, is the absence of a priori information on the location and types of singularities in the spatial computational region. To solve this problem it was proposed in [5, 6] for the first time to apply the methods of digital image processing for the detection of strong discontinuities in the numerical solutions of fluid dynamics problems. In [7, 3] these methods were augmented by the methods of digital pattern recognition in order to classify the detected singularities lines in types. The performance of the developed algorithms for the localization and classification of singularities was demonstrated in [3] on a number of two-dimensional aerodynamics problems: the transonic flow around the airfoil, the double

## Report Documentation Page

<b>Report Date</b> 23 Aug 2002	<b>Report Type</b> N/A	<b>Dates Covered (from... to)</b> -
<b>Title and Subtitle</b> Digital Diagnostics of Multiphase Flows by The Pattern Recognition Techniques		<b>Contract Number</b>
		<b>Grant Number</b>
		<b>Program Element Number</b>
<b>Author(s)</b>		<b>Project Number</b>
		<b>Task Number</b>
		<b>Work Unit Number</b>
<b>Performing Organization Name(s) and Address(es)</b> Institute of Theoretical and Applied Mechanics Institutskaya 4/1 Novosibirsk 530090 Russia		<b>Performing Organization Report Number</b>
<b>Sponsoring/Monitoring Agency Name(s) and Address(es)</b> EOARD PSC 802 Box 14 FPO 09499-0014		<b>Sponsor/Monitor's Acronym(s)</b>
		<b>Sponsor/Monitor's Report Number(s)</b>
<b>Distribution/Availability Statement</b> Approved for public release, distribution unlimited		
<b>Supplementary Notes</b> See also ADM001433, Conference held International Conference on Methods of Aerophysical Research (11th) Held in Novosibirsk, Russia on 1-7 Jul 2002		
<b>Abstract</b>		
<b>Subject Terms</b>		
<b>Report Classification</b> unclassified	<b>Classification of this page</b> unclassified	
<b>Classification of Abstract</b> unclassified	<b>Limitation of Abstract</b> UU	
<b>Number of Pages</b> 6		

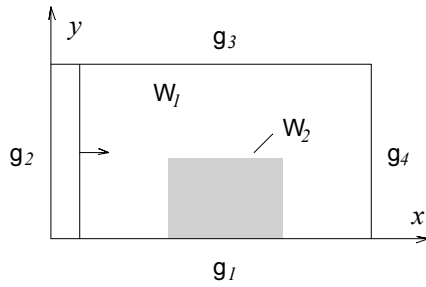
Mach reflection of a shock wave on a wedge, the supersonic flow in a channel with a lower wall backward-facing step. The pattern recognition methods described in [3] were applied in [8] for the diagnostics of the discontinuities structure in the problem of the shock wave diffraction around a planar wedge.

It should be noted that the methods of digital pattern recognition were applied in [3, 5 – 8] only for the diagnostics of pure gas flows. At the same time, as is known from the theory of two-phase flows of the mixtures of gas and solid particles, the shock waves as well as other singularities can arise in such flows, and the number of different types of singularities in two-phase flows even proved to be larger than in the case of pure gas flows [9, 10].

A generalization of the algorithms for digital localization and classification of singularities described in [2, 3, 5 – 8] is proposed in the present work for the case of two-phase flows of the mixtures of gas and solid particles. The examples of the diagnostics of specific flows are presented.

### The Problem of Shock Wave Interaction with a Cloud of Particles

Following [11] let us consider a rarefied cloud of solid spherical particles occupying the region  $\Omega_2$  (Fig. 1) at the initial moment of time  $t = 0$ . At some time  $t > 0$ , a shock wave (SW)



impinges from the left on the cloud of particles. In  $\Omega_1$  the gas flow is governed by the Euler equations, and in  $\Omega_2$  by the equations of discrete/continual model. Choosing the  $x$  axis along the SW propagation, and the  $y$  axis along a normal to the  $x$  axis let us write a system of the equations for a flow of a gas – particle mixture in planar case:

Fig. 1.

$$\frac{\partial f}{\partial t} + v_2 \frac{\partial f}{\partial x} + w_2 \frac{\partial f}{\partial y} + \frac{\partial}{\partial v_2} (a_x f) + \frac{\partial}{\partial w_2} (a_y f) + \frac{\partial}{\partial T_2} (qf) = 0,$$

$$f = f(t, x, y, v_2, w_2, r, T_2), \quad n = \int f dV, \quad m_2 = \frac{4}{3} \pi \int r^3 f dV,$$

$$dV = dv_2 dw_2 dr dT_2, \quad m_1 + m_2 = 1, \quad q = 2\pi\lambda r Nu \frac{T_1 - T_2}{c_s m_p},$$

$$a_x = \frac{v_1 - v_2}{\tau} - \frac{1}{\rho_{22}} \frac{\partial p}{\partial x}, \quad a_y = \frac{w_1 - w_2}{\tau} - \frac{1}{\rho_{22}} \frac{\partial p}{\partial y}, \quad \frac{1}{\tau} = \frac{3}{4} \left( \frac{\text{Re} \mu}{\rho_{22} d^2} \right) C_d(\text{Re}, M_{12}), \quad m_p = \frac{4}{3} \pi r^3 \rho_{22},$$

$$C_d(\text{Re}, M_{12}) = \left( 1 + \exp \left( - \frac{0.43}{M_{12}^{4.67}} \right) \right) \left( 0.38 + \frac{24}{\text{Re}} + \frac{4}{\sqrt{\text{Re}}} \right),$$

$$\begin{aligned}
\text{Re} &= \frac{\rho_{11} |\vec{v}_1 - \vec{v}_2| d}{\mu}, \quad M_{12} = \frac{|\vec{v}_1 - \vec{v}_2|}{c}, \quad c = \sqrt{\frac{\gamma p}{\rho_{11}}}, \\
\text{Nu} &= 2 + 0.6 \text{Re}^{0.5} \text{Pr}^{0.33}, \quad \text{Pr} = \frac{c_p \mu}{\lambda}, \quad \varepsilon_1 = c_v T_1, \\
\frac{\partial \varphi}{\partial t} + \frac{\partial F}{\partial x} + \frac{\partial G}{\partial y} + \Phi &= 0, \quad \rho_1 = \rho_{11} m_1, \quad p = (\gamma - 1) \rho_{11} \varepsilon_1, \\
\varphi &= \begin{pmatrix} \rho_1 \\ \rho_1 v_1 \\ \rho_1 w_1 \\ \rho_1 (\varepsilon_1 + (v_1^2 + w_1^2)/2) \end{pmatrix}, \quad F = \begin{pmatrix} \rho_1 v_1 \\ \rho_1 v_1^2 + p m_1 \\ \rho_1 v_1 w_1 \\ \rho_1 v_1 A_1 \end{pmatrix}, \quad G = \begin{pmatrix} \rho_1 w_1 \\ \rho_1 v_1 w_1 \\ \rho_1 w_1^2 + p m_1 \\ \rho_1 w_1 A_1 \end{pmatrix}, \quad \Phi = \begin{pmatrix} 0 \\ \Phi_1 \\ \Phi_2 \\ A_2 \end{pmatrix}, \\
A_1 &= \varepsilon_1 + \frac{p m_1}{\rho_1} + \frac{(v_1^2 + w_1^2)}{2}, \quad \rho_{22} = \text{const}, \\
A_2 &= v_1 \Phi_1 + w_1 \Phi_2 + p \left( \frac{\partial m_1}{\partial t} + v_1 \frac{\partial m_1}{\partial x} + w_1 \frac{\partial m_1}{\partial y} \right) - \rho_1 \Phi_3, \\
\Phi_3 &= \frac{1}{\rho_1} \int m_p \left( \frac{(v_1 - v_2)^2}{\tau} + \frac{(w_1 - w_2)^2}{\tau} - c_s q \right) f dV, \\
\Phi_1 &= -p \frac{\partial m_1}{\partial x} + \int m_p \frac{v_1 - v_2}{\tau} f dV, \quad \Phi_2 = -p \frac{\partial m_1}{\partial y} + \int m_p \frac{w_1 - w_2}{\tau} f dV.
\end{aligned} \tag{1}$$

Here the subscripts 1 and 2 denote the gas and particle parameters, respectively;  $f$  is the distribution function;  $v_1, w_1, \rho_{11}, \rho_1, T_1, p, \gamma, \varepsilon_1, m_1$  are the gas velocities along the  $x$  and  $y$ , the true density, mean density, temperature, pressure, the adiabatic exponent, the specific internal energy, and the volume concentration of gas;  $n$  is the number concentration of particles;  $v_2, w_2, a_x, a_y, \rho_{22}, r, T_2, m_2$  are the velocities and accelerations along the  $x$  and  $y$ , the true density, radius, temperature, and volume concentration of particles;  $\mu, \lambda, c_v, c$  are the viscosity, heat conduction, heat capacity, and sound velocity in gas;  $c_s$  is the specific heat of the particles material;  $\text{Re}, \text{Nu}, \text{Pr}$ , and  $M_{12}$  are the Reynolds, Nusselt, Prandtl, and Mach numbers.

The system of equations (1) was solved numerically on a desktop computer. The gas equations were solved on an Eulerian grid with the third order of accuracy, and the kinetic equation was solved in the Lagrange variables. The equations of paths and heat transfer of particles were integrated analytically at each time step. This has enabled us to increase the accuracy of the computation of particles and eliminated a limitation for the time step  $\tau \leq \rho_{11} d^2/\mu$ . The solid wall condition was set on  $\gamma_1$  for gas, and on  $\gamma_2, \gamma_3$ , and  $\gamma_4$  the symmetry condition was assumed. The mirror reflection condition was specified for particles on  $\gamma_1$ , and the condition for particles absorption was specified on  $\gamma_2, \gamma_3$ , and  $\gamma_4$  (see Fig. 1).

### The Algorithm for Localization and Classification of Singularities in Two-Phase Flow

As was shown in [9], in the case when the gas density is much smaller than the density of particles material, that is  $\rho_{11}/\rho_{22} \ll 1$ ,  $m_2 \ll 1$ , then one can neglect the variation of temperature and velocity of particles across the shock wave front. Then the relations are obtained on a shock wave in two-phase flow, which coincide with the Rankine — Hugoniot conditions in pure gas:

$$\begin{aligned} \rho_1^+ (v_{1n}^+ - D) &= \rho_1^- (v_{1n}^- - D); \\ v_{1\tau}^+ &= v_{1\tau}^-; \\ \rho_1^+ (v_{1n}^+ - D)^2 + p_1^+ m_1^+ &= \rho_1^- (v_{1n}^- - D)^2 + p_1^- m_1^-; \\ \varepsilon_1^+ + p_1^+ / \rho_{11}^+ + (u_{1n}^+ + u_{1\tau}^+)^2 / 2 &= \varepsilon_1^- + p_1^- / \rho_{11}^- + (u_{1n}^- + u_{1\tau}^-) / 2. \end{aligned} \quad (2)$$

The superscript “+” refers here to the medium state ahead of the discontinuity front, and the superscript “−” refers to the state behind the discontinuity front. Since the relations  $\rho_{11}/\rho_{22} \ll 1$ ,  $m_2 \ll 1$  are satisfied in the case of the problem of the interaction of a shock wave in gas with the coal dust cloud, one can use for the localization and classification of strong discontinuities in the given two-phase flow the algorithm, which was developed previously in [3, 7] for the case of pure gas flows. In this connection, we describe below only briefly the basic stages of this algorithm. These are the following two stages:

Stage I. Localization of lines of all discontinuities.

Stage II. The classification of the detected discontinuity lines in types with the aid of the test of the jump relations (2).

The procedure for localization of discontinuity lines consists of the following stages:

1. Computation of the gradient magnitude  $g_{ij}$  in all nodes  $(i, j)$  of the digital image for gas density  $\rho_{1ij}$ . For this purpose the formulas of the Sobel’s edge detector [3, 5 – 7] were used:

$$\begin{aligned} g_{ij} = & |(\rho_{1,i-1,j+1} + 2\rho_{1,i,j+1} + \rho_{1,i+1,j+1}) - (\rho_{1,i-1,j-1} + 2\rho_{1,i,j-1} + \rho_{1,i+1,j-1})| \\ & + |(\rho_{1,i+1,j+1} + 2\rho_{1,i+1,j} + \rho_{1,i+1,j-1}) - (\rho_{1,i-1,j+1} + 2\rho_{1,i-1,j} + \rho_{1,i-1,j-1})|. \end{aligned}$$

1. Thresholding.
2. Edge thinning.
3. Tracing contour segments.

As regards the algorithm for contour tracing, it was not yet realized in [3]. This algorithm was implemented in [12] to detect the boundaries of the multiply connected stability regions of difference schemes. Since the algorithm for tracing contour segments described in [12] is universal, we have applied it without changes for tracing the segments of discontinuity lines on the basis of the points of these discontinuities, which were detected at the foregoing stages. The above algorithm is based on the ideas for tracing contour segments, which were presented in [13, 14].

The classification of the lines found at stage I into types of discontinuities was performed at stage II with the aid of the sequential classification algorithm described in [3]. In this algorithm, all the conditions (2) on a discontinuity were verified sequentially. To identify the shock wave fronts also the condition for the entropy increase behind the shock wave front was checked. The algebraic relations valid on purely contact discontinuities and tangential discontinuities were checked, which are satisfied on the discontinuities of these types, cf. [3].

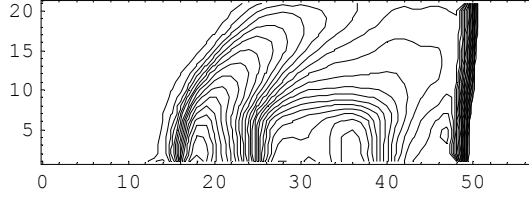


Fig. 2. The isolines of gas density  $\rho_1$ .

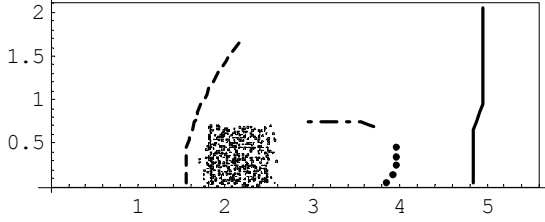


Fig. 3. The results of localization and classification of singularities in the gas phase of the two-phase flow: solid line is the normal shock wave, dashed line is the oblique shock wave, the dash-dot line is the tangential discontinuity, the black circles show a purely contact discontinuity.

The computation of two-phase flow and subsequent localization and classification of singularities were executed with the aid of the corresponding Fortran programs. Then the plotting of isolines of gas density (see Fig. 2) and the lines of various discontinuities (see Fig. 3) was carried out with the aid of a program written in the language of the software system Mathematica 4.1. Figure 2 shows the isolines of the gas density  $\rho_1$  at the moment of time when the shock wave has already passed through the cloud of particles. The gas parameters ahead of the SW correspond to  $\rho_{11}^0 = 1.3 \cdot 10^{-3} \text{ g/cm}^3$ ,  $T_1^0 = 293 \text{ K}$ ,  $p^0 = 1 \text{ atm}$ , the SW Mach number  $M_0 = 3.0$ . The initial volume concentration of particles in the dust cloud at  $t = 0$  is  $m_2^0 = 0.01$ . The density of coal particles  $\rho_{22} = 1.2 \text{ g/cm}^3$ , the particles diameter  $d = 100 \text{ }\mu\text{m}$ . Figure 2 shows 40 different isolines of the gas density. It can be seen that the isolines coalesce in the region of the impinging shock wave and the shock reflected from the particles cloud. The coalescence of isolines in the region of a contact discontinuity behind the cloud of particles is not so pronounced. This is related to the following two circumstances. First, a relatively crude grid of  $56 \times 21$  cells was used in the computations whose results are presented in Figs. 2 and 3. Second, the contact discontinuities are smeared more intensely than the shock waves while using the shock-capturing schemes [2, 3].

Figure 3 presents the results of the application of the above described algorithm for localization and classification of singularities in two-phase flows on the basis of shock-capturing computational results. It can be seen that the normal impinging shock wave becomes slightly curved after its passage through the cloud of particles. A contact discontinuity may be seen in gas between the cloud of particles and the shock wave. It is a purely contact discontinuity near the  $x$  axis and it goes over to a tangential discontinuity as the distance from the  $x$  axis increases. This tangential discontinuity separates the gas percolated through the cloud from the gas, which was located to the right of the cloud at the initial moment of time  $t = 0$  and then accelerated by the shock wave.

The cloud of particles was plotted in Fig. 3 as follows.  $N_0$  marker particles ( $N_0 \geq 1$ ) were assigned to the initial volume concentration of particles  $m_2^0$ , so that the  $(1/N_0)$ th fraction of the volume concentration of particles corresponds to each marker particle. Then, knowing the volume concentration of particles  $m_{2ij}^n$  in each cell  $(i, j)$ , we can find the number of corresponding marker particles  $n_{ij}$  in this cell by formula  $n_{ij} = [m_{2ij}^n N_0 / m_2^0]$ , where  $[a]$  is the integral part of the number  $a$ , which does not exceed  $a$ . The coordinates  $(x_{ijk}, y_{ijk})$  of marker particles in the  $(i, j)$  cell were found thereafter by formulas:  $x_{ijk} = (i - I + R) h_1$ ,  $y_{ijk} =$

$(j - 1 + R)h_2$ , where  $R$  is a pseudorandom quantity lying in the interval  $[0, 1]$ . This quantity was generated in the Mathematica 4.1 program with the aid of the built-in function **Random[]**. It can be seen from Fig. 3 that the cloud of particles at the time under consideration has not yet been deformed significantly in comparison with its initial shape.

#### REFERENCES

1. **Oran E.S., Boris J.P.** Numerical Simulation of Reactive Flow. New York: Elsevier, 1987.
2. **Vorozhtsov E.V., Yanenko N.N.** Methods for the Localization of Singularities in Numerical Solutions of Gas Dynamics Problems. Novosibirsk: Nauka, 1985.
3. **Vorozhtsov E.V., Yanenko N.N.** Methods for the Localization of Singularities in Numerical Solutions of Gas Dynamics Problems. New York: Springer-Verlag, 1990.
4. **LeVeque R.J.** Numerical Methods for Conservation Laws. Basel: Birkhäuser Verlag, 1992.
5. **Vorozhtsov E.V.** On Shock Localization in Difference Solutions with the Aid of the Sobel Edge Detector. Preprint, ITAM SB USSR Acad. Sci. Novosibirsk, 1985, No. 12.
6. **Vorozhtsov E.V.** On shock localization by digital image processing techniques // Computers and Fluids. 1987. Vol. 15, No. 1. P. 13 – 45.
7. **Vorozhtsov E.V.** On the classification of discontinuities by the pattern recognition methods // Computers and Fluids. 1990. Vol. 18, No. 1. P. 35 – 74.
8. **Bazarov S.B.** Application of image processing to the shock wave diffraction problem // 19<sup>th</sup> Intern. Sympos. on Shock Waves: Proc. Berlin, Heidelberg, Springer-Verlag, 1995. P. 113 – 139.
9. **Kiselev S.P., Ruev G.A., Trunyov A.P., Fomin V.M., Shavaliyev M.Sh.** Shockwave Processes in Two-Component and Two-Phase Media. Novosibirsk: Nauka, 1992.
10. **Kiselev S.P., Vorozhtsov E.V., Fomin V.M.** Foundations of Fluid Mechanics with Applications: Problem Solving Using Mathematica. Boston: Birkhäuser, 1999.
11. **Kiselev S.P., Kiselev V.P.** On the ignition of coal dust particles in shock waves // J. Appl. Mech. Tech. Phys. 1996. Vol. 36, No. 3. P. 31 – 37.
12. **Ganzha V.G., Vorozhtsov E.V.** Computer-Aided Analysis of Difference Schemes for Partial Differential Equations. New York: Wiley-Interscience, 1996.
13. **Nevatia R., Babu K.R.** Linear feature extraction and description // Computer Graphics and Image Processing. 1980. Vol. 13, No. 3. P. 257 – 269.
14. **Semenkov O.I., Ablameiko S.V., Bereishik V.I., Starovoitov V.V.** On the Processing and Mapping of Information in Raster Graphics Systems. Minsk: Nauka i tekhnika, 1989.